Biologic Effects of Dopamine on Tumor Vasculature in Ovarian Carcinoma[1,2]

Myrthala Moreno-Smith[*,3], Sun Joo Lee[†,3], Chunhua Lu[*], Archana S. Nagaraja[*], Guangan He[‡], Rajesha Rupaimoole[*], Hee Dong Han[*], Nicholas B. Jennings[*], Ju-Won Roh[§], Masato Nishimura[¶], Yu Kang[*], Julie K. Allen[*], Guillermo N. Armaiz[*], Koji Matsuo[*], Mian M. K. Shahzad[*], Justin Bottsford-Miller[*], Robert R. Langley[#], Steve W. Cole[**], Susan K. Lutgendorf[††], Zahid H. Siddik[‡] and Anil K. Sood[*,#,‡‡]

*Department of Gynecologic Oncology, The University of Texas MD Anderson Cancer Center, Houston, TX; †Department of Obstetrics and Gynecology, Konkuk University Hospital, Konkuk University School of Medicine, Seoul, South Korea; ‡Department of Experimental Therapeutics, The University of Texas MD Anderson Cancer Center, Houston, TX; §Department of Obstetrics and Gynecology, Dongguk University Ilsan Hospital, Goyang, South Korea; ¶Department of Obstetrics and Gynecology, The University of Tokushima Graduate School, Tokushima, Japan; #Department of Cancer Biology, The University of Texas MD Anderson Cancer Center, Houston, TX; **Department of Medicine, Division of Hematology and Oncology, University of California, Los Angeles School of Medicine, Los Angeles, CA; ††Departments of Psychology and Gynecology and the Holden Comprehensive Cancer Center, University of Iowa, Iowa City, IA; ‡‡Center for RNA Interference and Non-Coding RNA, The University of Texas MD Anderson Cancer Center, Houston, TX

Abstract

Chronic sympathetic nervous system activation results in increased angiogenesis and tumor growth in orthotopic mouse models of ovarian carcinoma. However, the mechanistic effects of such activation on the tumor vasculature are not well understood. Dopamine (DA), an inhibitory catecholamine, regulates the functions of normal and abnormal blood vessels. Here, we examined whether DA, an inhibitory catecholamine, could block the effects of

chronic stress on tumor vasculature and tumor growth. Exogenous administration of DA not only decreased tumor microvessel density but also increased pericyte coverage of tumor vessels following daily restraint stress in mice. Daily restraint stress resulted in significantly increased tumor growth in the SKOV3ip1 and HeyA8 ovarian cancer models. DA treatment blocked stress-mediated increases in tumor growth and increased pericyte coverage of tumor endothelial cells. Whereas the antiangiogenic effect of DA is mediated by dopamine receptor 2 (DR2), our data indicate that DA, through DR1, stimulates vessel stabilization by increasing pericyte recruitment to tumor endothelial cells. DA significantly stimulated migration of mouse 10T1/2 pericyte-like cells *in vitro* and increased cyclic adenosine monophosphate (cAMP) levels in these cells. Moreover, DA or the DR1 agonist SKF 82958 increased platinum concentration in SKOV3ip1 tumor xenografts following cisplatin administration. In conclusion, DA stabilizes tumor blood vessels through activation of pericyte cAMP–protein kinase A signaling pathway by DR1. These findings could have implications for blocking the stimulatory effects of chronic stress on tumor growth.

Introduction

There is growing recognition of the stimulatory effects of chronic stress on tumor growth. The sympathetic nervous system is activated in response to chronic stress, with resultant increases in stress hormones such as norepinephrine (NE) and epinephrine (E) [1,2]. We have recently demonstrated that both of these catecholamines are elevated in a sustained fashion in ovarian and other peritoneal tissues in preclinical models of chronic stress [3]. These hormonal increases were associated with greater tumor burden, which was mediated by increased tumor angiogenesis. The β-adrenergic cyclic adenosine monophosphate (cAMP) signaling pathway was identified as the underlying signaling pathway responsible for angiogenesis in these malignant ovarian tumors [3]. Recent evidence suggests that the third catecholamine, dopamine (DA), has an effect opposite to that of NE and E with regard to tumor angiogenesis, growth, and the development of ascites [4,5]. *In vivo* and *in vitro* studies have shown that DA, through its specific dopamine receptor 2 (DR2), inhibits tumor growth by suppressing the actions of vascular permeability factor/vascular endothelial growth factor A on both tumor endothelial cells and bone marrow–derived endothelial progenitor cells [6]. DA can also inhibit the mobilization of endothelial progenitor cells from the bone marrow [7]. We have previously described that DA levels are decreased in ovarian carcinomas from stressed mice and that DA replacement counteracts the stimulatory effects of NE and E on tumor growth by inhibiting tumor angiogenesis [8]. We have also demonstrated that DA replacement can block the stimulatory effects of sympathetic mediators on ovarian cancer growth [8]. However, the mechanisms by which DA affects tumor vasculature are not fully understood.

Our previous studies have shown that pericyte coverage was decreased in tumor vessels from stressed animals. Therefore, we wondered whether DA could block such stress-mediated effects. Pericytes are attached to endothelial cells and are critical for the development of a functional vascular network [9]. The exact molecular mechanisms mediating pericyte coverage are not fully understood and its biologic relevance in tumors is currently being investigated. Here, we examined whether DA could also block the adverse effects of chronic stress on tumor vasculature by stimulating pericyte recruitment and promoting tumor vessel maturation.

Materials and Methods

Reagents

DA, bromocriptine (DR2 agonist), eticlopride (DR2 antagonist), SKF 3839 (DR1 agonist), butaclamol (DR1 antagonist), KT 5720 [protein kinase A (PKA) inhibitor], H89 (PKA inhibitor), dibutyryl cAMP (dbcAMP; PKA activator), and NE were obtained from Sigma-Aldrich (Detroit, MI); recombinant human vascular endothelial growth factor was obtained from R&D Systems (Minneapolis, MN). Annexin V and TUNEL staining kits were purchased from Pharma BD (Franklin Lakes, NJ) and Promega (Madison, WI), respectively.

Cell Lines and Culture Conditions

The ovarian cancer cells (SKOV3ip1 and HeyA8) were maintained in RPMI 1640 supplemented with 15% FBS and 0.1% gentamicin sulfate (Gemini Bioproducts, Calabasas, CA) [10,11]. Murine pericyte-like cell line 10T1/2 (embryonic fibroblasts) was obtained from American Type Culture Collection (ATCC, Manassas, VA; CCL-226). Endothelial cells isolated from the ovary of the immortomouse (MOEC) [12] were maintained in Dulbecco's modified Eagle's medium with 10% FBS. Mouse pericyte-like cells (10T1/2) were maintained in Dulbecco's modified Eagle's medium with 10% FBS and glutamine. All *in vitro* experiments were conducted when cells were at 60% to 80% confluence, unless otherwise specified. For *in vivo* injections, cancer cells were trypsinized and centrifuged at 1000 rpm for 7 minutes at 4°C, washed twice, and reconstituted in Hank's balanced salt solution (Gibco, Carlsbad, CA).

Reverse Transcription–Polymerase Chain Reaction Analysis of DRs

Total RNA was isolated by using a Qiagen RNeasy Kit (Valencia, CA). cDNA was synthesized by using the SuperScript First-Strand Kit (Invitrogen, Eugene, OR) as per the manufacturer's instructions. cDNA was subjected to polymerase chain reaction (PCR) analysis using specific primer sequences for murine DRs (DR1–DR5). These primer sequences were designed on the basis of the reported National Center of Biotechnology Information nucleotide sequences using OligoPerfect software (Invitrogen). *β-Actin* was used as a housekeeping gene.

Chronic Stress Model and Treatment Schema

Female athymic nude mice (10 to 12 weeks old) were obtained from the US National Cancer Institute. All experiments were approved by the Institutional Animal Care and Use Committee of The University of Texas MD Anderson Cancer Center. The mice were experimentally stressed by being restrained for 2 hours everyday using a well-characterized restraint system in which periodic immobilization induces high levels of hypothalamic-pituitary-adrenal and sympathetic nervous system activities, characteristic of chronic stress [3]. Ovarian cancer cells were injected intraperitoneally (i.p.) into the mice 7 days after starting daily stress. Then, the mice were further divided into treatment groups (10 animals/group) as follows: 1) phosphate-buffered saline (PBS; control), 2) DA (75 mg/kg daily i.p.), 3) DA plus butaclamol (DR1 antagonist; 1.5 mg/kg daily i.p.), and 4) DA plus eticlopride (DR2 antagonist; 10 mg/kg daily i.p.). Following 3 weeks (SKOV3ip1 model) and 2 weeks (HeyA8 model) of treatment, the mice were killed and their tumors were excised. Tumor weight and number of tumor nodules were recorded, and tumor and relevant tissue samples were collected.

Concentration of Platinum in Tumors Following Cisplatin Administration

Female nude mice bearing SKOV3ip1 tumors (~3 weeks after cell implantation) were injected (i.p.) daily for 6 days with PBS, DA (75 mg/kg), or the DR1 agonist SKF 82958 (1 mg/kg), and 30 minutes after the final injection, mice also received 7 mg/kg cisplatin (i.p.). Animals were sacrificed 6 hours later and samples (20–120 mg) from tumor (from three different peritoneal sites), left kidney cortex, and liver were excised, rinsed in ice-cold PBS, gently blotted dry, weighed, and processed for platinum (Pt) determination by flameless atomic absorption spectrophotometry, as previously described [13,14]. Briefly, samples were solubilized overnight in two volumes of benzethonium hydroxide at 55°C, acidified with 0.3 N HCl to give a final tissue concentration of 12.5 mg/ml, and analyzed for Pt levels against standard curves prepared with control tissue and a certified Pt standard (Sigma). The averaged Pt level in tumor samples are presented as tumor/kidney and tumor/liver ratios to normalize for any variation in cisplatin absorption and distribution affected by tumor mass.

Analysis of Angiopoietin 1 mRNA Expression

A quantitative reverse transcription (RT)–PCR assay was used to measure angiopoietin 1 (Ang1) mRNA in RNA extracted from SKOV3ip1 tumor tissues using primers designed for Ang1 isoform 1: sense, 5′-CACAACTATGATGATTCG-3′; antisense, 5′-TTCACATA-ACTACCACTTA-3′, and for Ang1 isoform 2: sense, 5′CACAACTAT-GATGATTCG-3′; antisense, 5′TTCACATAACTACCACTTA-3′. Total RNA was isolated using a Qiagen RNeasy Kit. RT of 1 µg of total RNA was performed using the Verso cDNA (Thermo Scientific, Albany, NY). *18S* was using as a housekeeping gene to normalize Ang1 mRNA levels. Relative quantification values were normalized to a housekeeping gene (*18S*) according to the $2^{-\Delta\Delta Ct}$ comparative threshold cycle (Ct) method [15].

cAMP Determination

The effect of DA on cAMP accumulation was examined by exposing cells to 0, 10, and 50 µM DA for 30 minutes at 37°C. cAMP levels were measured in total cell lysates using an enzyme immunoassay kit (Biomol, Plymouth, PA).

Cell Migration Assay

Migration into a gelatin-coated membrane matrix was assessed using the Membrane Invasion Culture System, as previously described [16]. A total of 1.5×10^5 SKOV3ip1 cells were loaded into the upper chamber in media only or in media containing the stimulant of interest. The following reagents were used in these experiments: DA (10 µM); NE (10 µM); PDGF-BB (10 ng/ml); SKF38393, butaclamol, and eticlopride (50 µM); and KT 5720, H89, and dbcAMP (10 µM). Cells were allowed to invade in a humidified incubator for 5 hours. Cells that had invaded through the basement membrane were collected, stained, and counted by light microscopy in five random fields (original magnification, ×200) per sample.

Western Blot and Immunoprecipitation Analyses

Western blot analysis was performed as previously described [17]. Briefly, lysates from cultured cells were prepared using modified RIPA buffer, and the protein concentrations were determined using a BCA Protein Assay Reagent Kit (Pierce Biotechnology, Rockford, IL). Protein lysates were subjected to 10% sodium dodecyl sulfate–polyacrylamide gel electrophoresis separation and transferred to a nitrocellulose membrane. Blots were probed with primary antibodies specific for DR1 and DR2 (Santa Cruz Biotechnology, Delaware, CA) and HRP-conjugated secondary antibody (Amersham, Piscataway, NJ) and subsequently developed with an enhanced chemiluminescence detection kit (ECL; Pierce Biotechnology). To confirm equal protein loading, membranes were stripped and reprobed with an anti–β-actin antibody (Sigma-Aldrich). To examine the association between Gαs protein and mDR1, pericyte cells were exposed to 10 µM DA for 0, 10, and 20 minutes at 37°C. Cell lysates were then prepared and immunoprecipitated with DR1 antibody (Santa Cruz Biotechnology) at 4°C for 14 hours. Immunocomplexes were captured with 2% protein A agarose beads (Upstate, Lake Placid, NY). Protein was eluted in reducing sample Laemmli buffer, subjected to 10% sodium dodecyl sulfate–polyacrylamide gel electrophoresis separation and transferred to a nitrocellulose membrane. Anti-Gαs (Abcam, Cambridge, MA) was used as primary antibody. Immunodetection of Gαs protein was performed as described above.

Immunohistochemical Analysis

Analysis of microvessel density (MVD) and assessment of tumor and endothelial cell apoptosis were performed as previously described [12,17–19]. Dual immunofluorescence staining for CD31 (red) and desmin (green) was performed as previously described [20]. Briefly, frozen tumor sections were fixed in cold acetone for 30 minutes and blocked with a protein blocker (4% fish gel). These sections were then probed with CD31 antibody (1:500; BD Pharmingen, San Diego, CA) at 4°C overnight. After washing with PBS, the sections were incubated with Alexa 594–conjugated anti-rat antibody (1:1000; Invitrogen) for 1 hour at room temperature. After extensive washing with PBS, the samples were then probed with anti-desmin antibody (1:400; DakoCytomation, Copenhagen, Denmark) for 2 hours, followed by washing with PBS and incubation with Alexa 488–conjugated anti-rabbit antibody (1:1000; Invitrogen) for 1 hour at room temperature. The samples were counterstained with Hoechst. Vessels with at least 50% coverage of associated desmin-positive cells were considered positive for pericyte coverage. Double immunofluorescence for DR1/G protein signaling 5 (RGS5) and for DR1/desmin was performed in frozen tissue sections as follows: After acetone fixation and blocking

with gelatin (4%), tissues were incubated with rabbit DR1 antibody (Santa Cruz Biotechnology; 1:100) at 4°C overnight. Samples were washed in PBS and incubated with blocking solution for 10 minutes and then with a goat anti-rabbit Alexa 488 antibody (1:1000) for 1 hour. Afterward, tissues were processed for the detection of RGS5 and desmin, as previously described [18,20]. Dual immunofluorescence staining for Ang1/RGS5 in frozen tumor tissues was performed following the procedure described above and using primary antibodies: rabbit anti-Ang1 antibody and goat anti-RGS5 (Santa Cruz Biotechnology).

Immunofluorescence and Confocal Microscopy

Immunofluorescence microscopy was performed using a Zeiss Axioplan fluorescence microscope (Carl Zeiss, Inc, Thornwood, NY) equipped with a 100-W Hg lamp and narrow band-pass excitation filters. Representative images were obtained using a cooled charge-coupled device Hamamatsu C5810 camera (Hamamatsu Photonics, Bridgewater, NJ) and Optimas software (Media Cybernetics, Silver Spring, MD). Confocal fluorescence images were collected using 20× objectives on a Zeiss LSM 510 laser scanning microscopy system (Carl Zeiss Inc) equipped with a motorized Axioplan microscope, argon laser (458/477/488/514 nm, 30 mW), HeNe laser (413 nm, 1 mW and 633 nm, 5 mW), LSM 510 control and image acquisition software, and appropriate filters (ChromaTechnology Corp, Brattleboro, VT). Composite images were constructed with Photoshop software (Adobe Systems, Inc, Mountain View, CA).

Statistical Analysis

Continuous variables were compared using Student's t test (between two groups) or analysis of variance (for all groups) if the variables were normally distributed and the Mann-Whitney rank sum test if the distributions were nonparametric. For the *in vivo* therapy experiments, 10 mice were used in each group, and a $P < .05$ on two-tailed testing was considered significant. To control for the effects of multiple comparisons, a Bonferroni adjustment was made; for that analysis, a P value $\leq .017$ was considered statistically significant.

Results

Expression of DA and β-Adrenergic Receptors in Murine Pericyte-Like Cells and in MOEC

Because DA can signal through multiple receptors, we first examined the RNA expression of DRs (mDR1–mDR5) in mouse 10T1/2 pericyte-like cells and in MOEC (Figure W1A). All five DRs were detected in both murine cell lines. DR1 and DR2 are the prototypes of the DR1 and DR2 subfamily of DRs, which mediate stimulatory and inhibitory effects in cells, respectively. Protein expression of mDR1 and mDR2 was confirmed by Western blot analysis in MOEC and 10T1/2 cells (Figure W1B). RNA expression of the β-adrenergic receptors ADRB1 and ADRB2 was also detected in both cell lines (Figure W1C).

DA Inhibits Stress-Mediated Tumor Growth and Stimulates Pericyte Coverage of Tumor Vasculature

On the basis of the known antiangiogenic effects of DA, we assessed the biologic consequences of DA in the context of chronic stress using a well-characterized daily restraint stress model. SKOV3ip1 tumor–

bearing nude mice ($n = 10$ mice per group) were treated according to the following groups: 1) control PBS, 2) DA, 3) DA + butaclamol (DR1 antagonist), or 4) DA + eticlopride (DR2 antagonist), under both no stress and stress conditions. Consistent with prior results, daily restraint increased tumor growth by 2.2-fold ($P < .001$; Figure 1A). While DA had no significant effect on tumor growth in the absence of stress, in mice exposed to daily restraint stress, DA treatment resulted in a 78% reduction in tumor growth compared to control ($P < .01$). A 44% reduction in the number of tumor nodules ($P < .05$) was also observed with DA treatment (Figure 1A). The inhibitory effect of DA on tumor growth was abrogated by the addition of the DR2 antagonist eticlopride but not the DR1 antagonist butaclamol. Given the known effects of catecholamines on angiogenesis, we examined MVD in the SKOV3ip1 tumors harvested from the treatment groups. In stressed mice, DA treatment resulted in a significant decrease of MVD compared to controls ($P < .05$; Figure 1A). This effect was also abrogated by DA plus eticlopride (DR2 antagonist) treatment but not by DA plus butaclamol (DR1 antagonist). This finding confirmed that the inhibitory effect of DA on angiogenesis is mediated by DR2. Tumor vessels with at least 50% coverage of associated desmin-positive cells were considered positive for pericyte coverage. In stressed mice, daily DA treatment resulted in a significant increase in pericyte coverage compared to the control group (two-fold; $P < .001$). This effect was abrogated by the addition of butaclamol to DA treatment (44%; $P < .01$) but not by DA plus eticlopride treatment (Figure 1A). This finding suggests that DA stimulates pericyte coverage through DR1. To determine the consistency of the observed effects, we used the HeyA8 ovarian cancer model. The effects of DA on tumor growth and MVD were similar to those described above for the SKOV3ip1 model (Figure 1B). In the HeyA8 model, DA increased pericyte coverage by 3.8-fold ($P < .001$), which was abrogated by addition of butaclamol (Figure 1B). Representative images of CD31/desmin staining of tissues from the different treatment groups (nonstressed and stressed mice) are shown in Figure 1C. Collectively, these data suggest that DA acts through DR1 to stimulate pericyte recruitment to tumor endothelial cells. To further examine the signaling pathway by which DA stimulates tumor vessel maturation, we evaluated pericyte coverage of SKOV3ip1 tumor tissues from mice treated with DA, DR1 agonist SKF 82958, and DR2 agonist parlodel. Tumor tissues from mice treated with DA and SKF 82958 revealed a significantly increased extent of pericyte coverage compared to the control group. Tissues from the parlodel group showed an increase in pericyte coverage; however, this increase was not statistically significant compared to controls (Figure W2).

Next, we examined the impact of DA on tumor hypoxia. For this purpose, frozen sections of SKOV3ip1 tumors from stressed mice were immunostained for carbonic anhydrase 9 (CA9). Figure W3 shows representative images (100×) from SKOV3ip1 tumor tissues stained for CA9. Tumor tissues from mice treated with DA revealed reduced areas of hypoxia in comparison with tumor tissues from nontreated (NT) stressed mice.

DA or SKF 82958 Increases Tumor Cisplatin Concentration and Enhances the Efficacy of Cisplatin Therapy

Pt concentration was determined in SKOV3ip1 tumor tissues 6 hours after cisplatin administration when tissue distribution of this Pt drug has stabilized [21]. The present study indicates that tumor levels of Pt are generally lower than in the liver or kidney, and this is apparent from the tumor/liver (Figure 2A) and tumor/kidney ratios
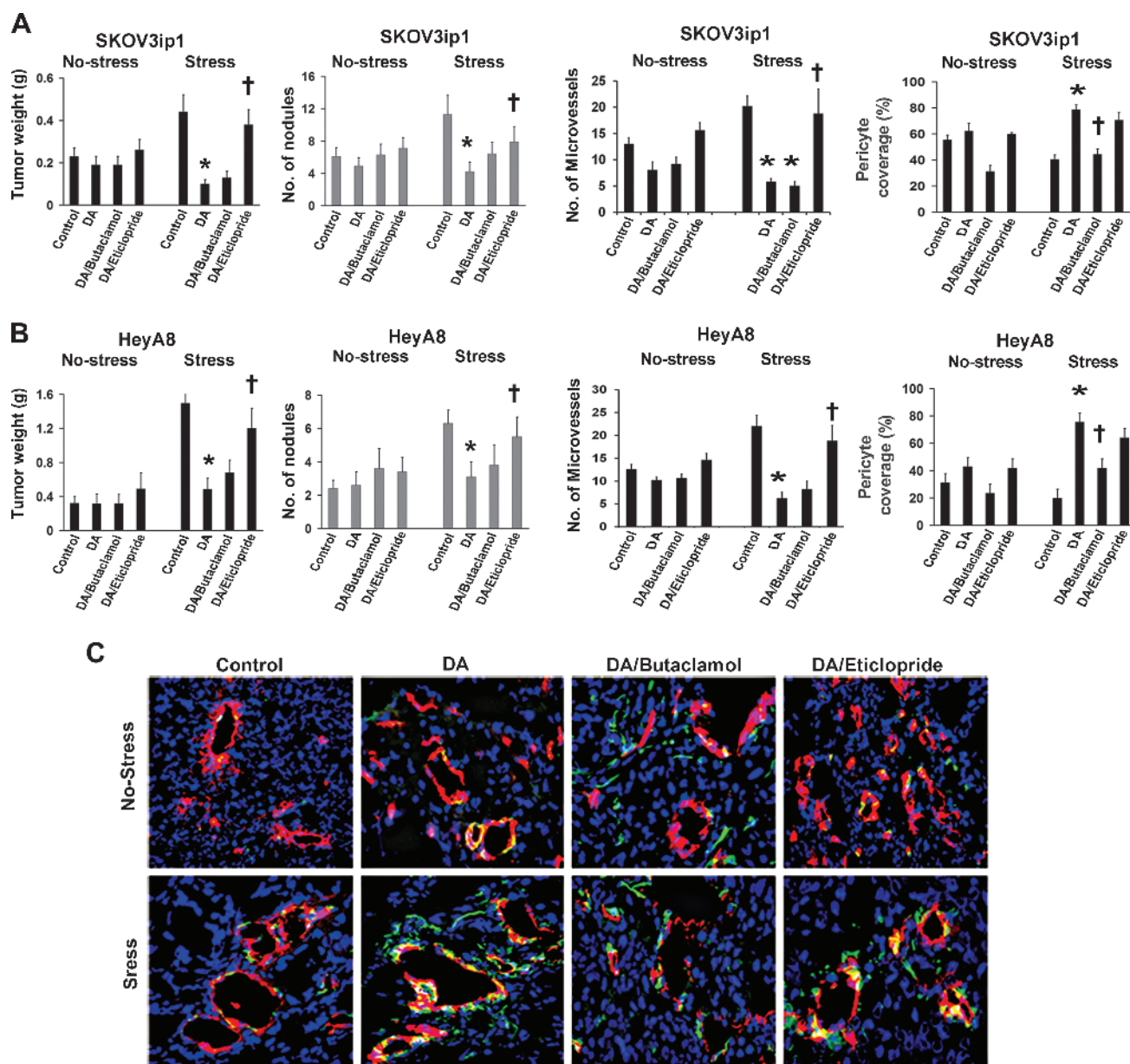
Figure 1. DA decreases stress-stimulated angiogenesis through DR2 and increases pericyte coverage through DR1. (A and B) Tumor weight and tumor nodules in nonstressed and stressed mice bearing SKOV3ip1 and HeyA8 tumors treated with PBS (control), DA, DA + butaclamol, or DA + eticlopride. DA significantly blocked tumor growth and reduced the number of tumor nodules in stressed mice from both ovarian cancer models. This effect was abrogated by the combined treatment of DA + eticlopride. Data are the means ± SE; $n = 10$ mice/group. *$P < .05$ compared with stress controls, [†]$P < .05$ compared to DA-treated mice. MVD was significantly decreased by DA treatment in SKOV3ip1 and HeyA8 tumor tissues of stressed mice (*$P < .05$ compared with stress controls). DA + eticlopride treatment significantly reversed DA inhibitory effect on MVD compared with DA-treated mice ([†]$P < .05$), which was evaluated by immunohistochemical analysis of CD31 (3,3′-diaminobenzidine) staining. Microvessels were counted in five fields (200×) of each tissue sample ($n = 5$). Values are means ± SE. Compared with nonstressed mice, pericyte coverage of tumor endothelial cells was significantly increased by DA treatment in tumor tissues (SKOV3ip1 and HeyA8) of stressed mice (*$P < .001$). The combined treatment of DA + butaclamol significantly reversed the stimulatory effect of DA on pericyte coverage ([†]$P < .01$). (C) Representative images (200×) from tumor tissues of the different mouse groups stained for CD31 (vessels—red fluorescence) and desmin (pericytes—green fluorescence). Vessels with at least 50% coverage of associated desmin-positive cells were considered positive for pericyte coverage. Percentage of tumor vessels with pericyte coverage was evaluated in five fields (200×) of each tissue sample ($n = 5$). Values are means ± SE.

(Figure 2B) of <0.2. However, both DA and the DR1 receptor agonist SKF 82958 increased the ratio two-fold or more ($P < .05$ and $P < .001$), and this indicates that these vascular stabilizing agents selectively increase Pt levels in the tumor. To determine whether DA or SKF 82958 increase the efficacy of cisplatin in inhibiting tumor

growth, SKOV3ip1 tumor–bearing stressed mice ($n = 5$ mice per group) were treated according to the following groups: 1) control PBS, 2) cisplatin, 3) cisplatin + DA, or 4) cisplatin + SKF 82958 and SKF 82958 alone. Compared to the control group, all treatment groups significantly inhibited tumor growth. The combined therapy of
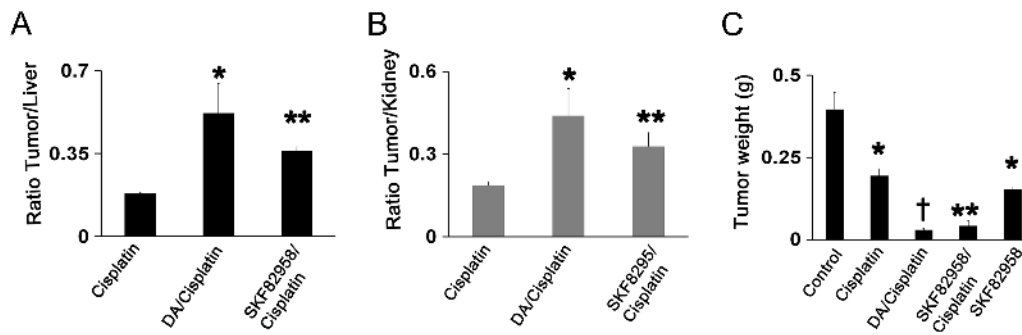
Figure 2. DA or SKF 82958 increases tumor cisplatin concentration and enhance the efficacy of cisplatin therapy. Nude stressed mice bearing SKOV3ip1 tumors treated with DA or DR1 agonist SKF 82958 for 6 days show significantly increased concentration of intratumoral cisplatin 6 hours after cisplatin injection. The averaged Pt level in tumor samples are presented as (A) tumor/liver and (B) tumor/kidney ratios to normalize for any variation in cisplatin absorption and distribution affected by tumor mass ($n = 5$; values are means $\pm$ SE; $*P < .05$; $**P < .001$). (C) Compared to the control group, all treatment groups significantly inhibited tumor growth, $*P < .01$; $**P < .001$; $^{\dagger}P < .0001$; the combined therapy of cisplatin + DA and cisplatin + SKF 82958 significantly increased the cisplatin efficacy by six-fold and five-fold, respectively ($n = 5$; values are means $\pm$ SE).

cisplatin + DA and cisplatin + SKF 82958 significantly increased the cisplatin efficacy by six-fold and five-fold, respectively (Figure 2*C*).

DA Treatment Does Not Affect Ang1 Expression in Ovarian Cancer Tumors

Given the importance of Ang1 as a signal for blood vessel stabilization [22–24], we also examined Ang1 expression in SKOV3ip1 tumor tissues from stressed mice treated with DA or DR1 and DR2 agonists. The results from these studies showed no significant changes in the mRNA and protein expression of Ang1 in tumor tissues from all treatment groups compared to the control group (Figure W4). This finding suggests that in ovarian carcinomas, Ang1 expression is not involved in the DA-stimulated effect on pericyte coverage and tumor vessel stabilization.

Catecholamines Affect Migration of Pericytes

Considering the *in vivo* effects of DA, that is, the promotion of pericyte coverage of tumor vasculature in stressed mice, we next analyzed the *in vitro* effects of DA, NE, DA plus NE, DA plus DR1 and DR2 antagonists, and the DR1 agonist SKF38393 in 10T1/2 cells. PDGF-BB was used as a positive control for stimulation of pericyte migration. Compared to NT cells, 10 μM DA significantly increased (1.5-fold; $P < .001$) the number of migrating pericytes (Figure 3). In contrast, 10 μM NE showed the opposite effect, significantly decreasing pericyte migration (30%; $P < .01$). In the presence of both DA and NE, pericyte migration was significantly greater, not only compared to NT cells (73%; $P < .001$) but also compared to DA treatment alone (20%; $P < .01$). The combined treatment of DA plus butaclamol (50 μM; DR1 antagonist) significantly abrogated the stimulatory effect of DA on pericyte migration (35%; $P < .001$). However, DA plus eticlopride (50 μM), a DR2 antagonist, did not reverse the DA effect. The DR1 agonist SKF38393 and PDGF-BB both stimulated migration (by 1.6-fold and 1.9-fold, respectively) compared with NT cells (Figure 3). These data further suggest that stimulation of pericyte migration by DA is mediated specifically through DR1. Migration of MOEC was also examined under the experimental conditions described above. In the presence of DA, migration of MOEC decreased, but treatment with NE and DA plus

NE did not induce significant changes in MOEC migration compared to NT cells (Figure W5).

DA and NE Regulate cAMP Levels in 10T1/2 Cells

DA, acting through G protein–coupled receptors, exerts stimulatory (through DR1 and DR5) or inhibitory (through DR2, DR3, and DR4) effects on adenylate cyclase, leading to increased or decreased cAMP levels, respectively. However, NE induces changes in cAMP production through α- or β-adrenergic receptors. Thus, cAMP levels in cells are regulated by activation of both dopaminergic and adrenergic receptors. We examined the effects of DA and NE on cAMP production in 10T1/2 cells at different time points (10, 20,
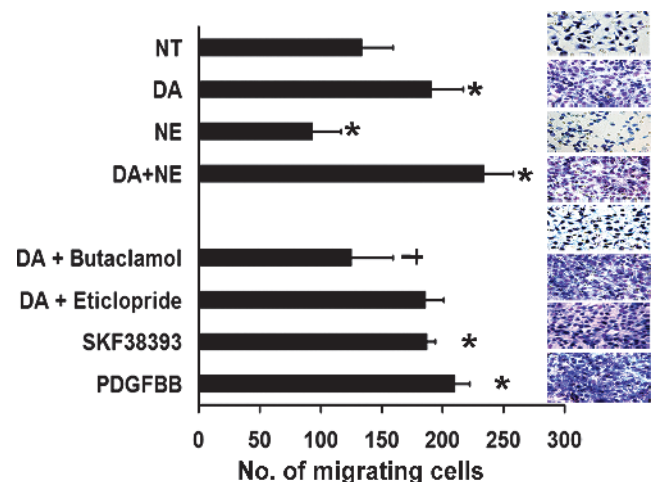

Figure 3. Effect of DA and various DA agonists and antagonists on 10T1/2 pericyte cells. DA and the DR1 agonist SKF38393 significantly stimulated 10T1/2 cell migration ($*P < .05$ compared with NT cells); butaclamol, a DR1-specific antagonist, abrogated the DA stimulatory effect on pericyte migration ($^{\dagger}P < .05$ compared with DA-treated cells), whereas eticlopride, a DR2-specific antagonist, did not affect cell migration. Representative images (200×) from pericyte cells were treated with the different compounds. Values are means $\pm$ SE of three independent experiments.
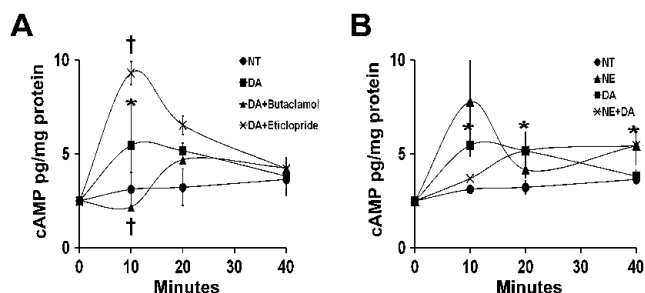
Figure 4. cAMP levels in 10T1/2 cells are regulated by DA and NE through DRs and adrenergic receptors. (A) DA exposure for 10 minutes resulted in a 1.8-fold (*$P < .05$) increase in cAMP levels compared with NT cells. This DA stimulatory effect was reversed by DA + butaclamol treatment ($^{†}P < .05$). In contrast, DA + eticlopride induced a greater accumulation of cAMP by inhibiting the DR2-mediated suppressive effect on cAMP production. After long exposure (40 minutes), there was no longer an effect of DA, and cAMP levels were similar to those in NT cells. (B) After 10 minutes of exposure, NE and DA alone increased cAMP levels by 2.5-fold and 1.8-fold (*$P < .05$), respectively. NE + DA treatment showed a 1.2-fold increase of cAMP levels. After 20 to 40 minutes of exposure, cAMP levels decreased in all three cell treatments. At 40 minutes of exposure, cAMP accumulation in DA-treated cells was similar to that in NT cells. In contrast, cAMP levels remained increased (1.6-fold) in both NE− and NE + DA–treated cells compared to NT cells (*$P < .01$).

and 40 minutes) after DA exposure. DA (10 μM) resulted in a 1.8-fold ($P < .05$) increase in intracellular cAMP levels after 10 minutes of incubation (Figure 4A). This stimulatory effect was abrogated by the DR1 antagonist butaclamol (Figure 4A). Exposure of 10T1/2 cells to DA plus the DR2 antagonist eticlopride resulted in a 3.5-fold increase in cAMP levels after 10 minutes of exposure. cAMP levels then decreased at 20 and 40 minutes after treatment. The effects of NE and NE plus DA were also examined in 10T1/2 pericyte-like cells (Figure 4B). At 10 and 40 minutes after NE (10 μM) exposure, cAMP levels were 2.5-fold and 1.6-fold higher, respectively, than in NT cells. Increases in cAMP levels of 1.2-fold, 1.6-fold, and 1.6-fold were identified in the presence of NE plus DA at 10, 20, and 40 minutes, respectively. These results indicate that DA increases intracellular cAMP levels in 10T1/2 cells through DR1. This suggests that DA acts through the DR1-cAMP signaling pathway to exert its *in vivo* stimulatory effects on pericyte recruitment to tumor endothelial cells. In the presence of NE plus DA, cAMP levels remained higher at all exposure times compared to those in NT cells (Figure 4B). These data further suggest that in stressed mice treated with DA, the stimulatory effects of NE and DA on cAMP production lead to consistently elevated cAMP levels that promote pericyte coverage and maturation of tumor vessels.

DA Stimulates Pericyte Recruitment through a DR1-cAMP-PKA Signaling Pathway

Our data described above indicated the potential role of DR1 in the DA-mediated stimulation of pericyte migration. To further address this question, we examined the association between DR1 and Gαs in the absence or presence of DA. The binding of DR1 to Gαs protein was 1.5-fold greater in cells treated with DA for 10 minutes than in NT cells. Figure 5A shows a representative image from three independent immunoprecipitation experiments. This finding further

points to the DR1-Gαs-cAMP signaling pathway for the impact of DA on pericyte function. DR1 and Gαs protein were detected in 10T1/2 cells by immunofluorescence staining in the absence and presence of DA (Figure 5B). Pericytes exposed to DA for 10 minutes showed an elongated, fibroblastic morphology compared to untreated cells. This change of cell morphology suggests that DA stimulates rearrangement of the cytoskeleton before pericyte migration. The localization of DR1 in pericytes was confirmed in 10T1/2 cells by double immunofluorescence staining for detection of RGS5 (pericyte marker) and DR1 (Figure 5C). In addition, colocalization of DR1 with desmin was detected in SKOV3ip1 tumors immunostained for desmin and DR1 (Figure 5C).

To determine whether activation of PKA is essential for stimulating pericyte migration after the activation of the DR1-cAMP signaling pathway by DA, we analyzed the effect of PKA inhibitors such as H89 and KT5720 on 10T1/2 cell migration. In combination with DA, each PKA inhibitor (10 μM) significantly abrogated the stimulatory effect of DA on pericyte migration (25–30%; $P < .05$). dbcAMP, a PKA activator, was used as a positive control for pericyte migration (Figure 5D).

Discussion

The key finding from this work is that DA, an antiangiogenic neurotransmitter, promotes maturation of ovarian cancer vasculature by enhancing pericyte recruitment to tumor endothelial cells during chronic stress. Tumors from mice exposed to chronic stress show numerous and tortuous immature blood vessels. In a previous study [8], we reported that DA, acting through DR2, blocked the stimulatory effects of chronic stress on ovarian cancer growth by inhibiting tumor angiogenesis and stimulating tumor cell apoptosis. These effects were mediated by inhibition of Src activation. Here, we show that DA replacement also promotes the normalization of tumor vasculature in ovarian cancer stress models and allows greater uptake of cisplatin. Our studies indicate that DA treatment counterbalances the negative effects of stress hormones and remodels the tumor vasculature. It is likely that that under stress conditions, tumor cells might be more responsive to DA replacement due to depletion of endogenous DA under such conditions.

The physiological actions of DA are mediated by at least five distinct G protein–coupled receptor subtypes. Two DR1-like receptor subtypes (DR1 and DR5) couple to the Gαs, activate adenylate cyclase, and increase cAMP levels. The other receptor subtypes belong to the DR2-like subfamily (DR2, DR3, and DR4) and are prototypic of G protein–coupled receptors that inhibit adenylate cyclase and decrease cAMP production. The MOEC and 10T1/2 cells tested in this work showed expression of DR1- and DR2-like DRs, indicating that DA might regulate stimulatory and/or inhibitory processes in these cells. Previous studies suggest that some antiangiogenic agents can also transiently "normalize" the abnormal structure and function of tumor vasculature to make it more functional for oxygen and drug delivery [25–27]. The transient normalization of tumor vessels produces a temporary increase in oxygen and nutrient delivery for cancer cells that surround these "normalized" vessels. Theoretically, such changes might be expected to enhance the proliferation of these cells and, hence, to accelerate tumor growth, but this notion is not supported by published data [25]. Drugs that induce vascular normalization can alleviate hypoxia and may increase the efficacy of conventional cancer therapies. Therefore, a better understanding of the molecular and cellular mechanisms of vascular normalization could lead to more
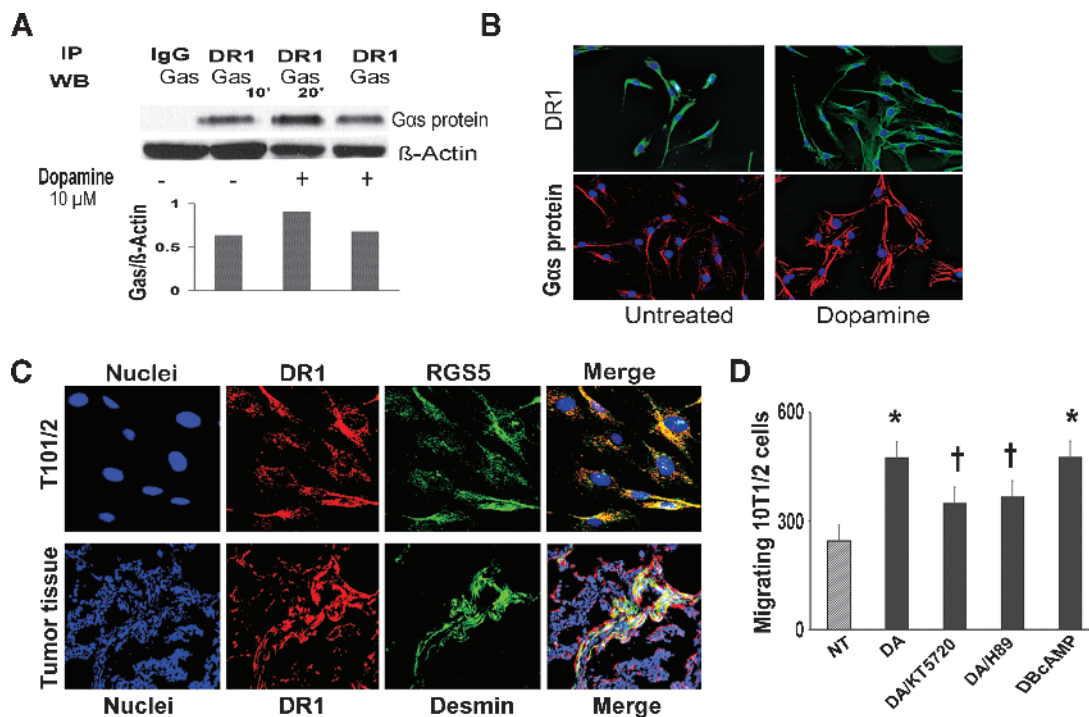
Figure 5. DA stimulates pericyte recruitment through DR1-cAMP-PKA signaling pathway. (A) DA induces association of DR1 to Gαs protein. 10T1/2 pericyte cells were exposed to DA (10 μM) for 10 and 20 minutes. Pericyte lysates were then immunoprecipitated with DR1 antibody and analyzed by Western blot analysis. Gαs was immunodetected using a specific anti-Gαs antibody (Abcam). DA caused a 1.5-fold higher interaction between DR1 and Gαs after 10 minutes of exposure compared with untreated cells. The densitometric data were normalized to a loading control (β-actin from original lysate) and are representative of two independent experiments. (B) Immuno-fluorescence images (200×) from untreated and 10T1/2 cells exposed to DA (10 μM) for 10 minutes and stained for DR1 and Gαs protein. Pericytes exposed to DA for 10 minutes showed an elongated, fibroblastic morphology compared to untreated cells. (C) Confocal images (200×) from 10T/12 cells revealing colocalization of DR1 (red fluorescence) with RGS5 (green fluorescence) and colocalization of mDR1 (red fluorescence) with desmin-positive cells (green fluorescence) in SKOV3ip1 tumor tissues. Yellow areas confirm the expression of mDR1 in 10T/12 cells and in tumor pericytes. (D) DA and PKA activator dbcAMP caused a two-fold increase in pericyte migration. PKA inhibitors KT5720 and H89 at 10 μM abrogated (25–30%) the stimulatory effect of DA on pericyte migration ($^{\dagger}P < .05$).

effective therapies for not only cancer but also other diseases with abnormal vasculature.

The second messenger cAMP and its effector, PKA, mediate the regulation of many processes, including glycogenolysis, ion transport, gene transcription, and cell proliferation and differentiation [28–30]. Increased levels of intracellular cAMP also cause reorganization of the actin cytoskeleton in REF52 fibroblasts [31] and a marked alteration of epithelial cells [32]. Our study demonstrates that DA, through DR1, promotes pericyte migration *in vitro* and pericyte recruitment to tumor endothelial cells *in vivo*. Butaclamol, a DR1-specific antagonist, abrogated the DA-stimulated effect on pericytes under both experimental conditions. This DR1-mediated normalization of vasculature by DA is important for antitumor drug distribution to the tumor, and this was clearly seen with cisplatin, which is likely to enhance antitumor effects. More importantly, the increase in tumor Pt levels was selective, and not observed in liver and kidney, which is likely to increase the therapeutic index. Similar effects of DA on increased uptake of 5-fluorouracil have also been reported [24]. Mechanistic studies in the present manuscript indicated that the cAMP-PKA signaling pathway is involved in the DA-mediated effect on pericytes. 10T1/2 pericyte-like cells treated with DA showed increased levels of cAMP and greater pericyte migration. In addition, cAMP levels and pericyte migration were even greater in the presence of both DA and NE. This experimental condition mimics the *in vivo*

scenario of chronically stressed mice treated with DA and suggests that NE reinforces the DA remodeling effect on tumor vasculature during chronic stress. The mechanism of this NE effect was not addressed in this study, but a potential explanation is that NE, by acting through the β-adrenergic pathway, could increase cAMP levels, which would stimulate pericyte migration. However, the question of why NE alone does not promote pericyte recruitment remains unanswered. It is conceivable that DA also activates additional signaling pathways that are not triggered by NE and contribute to the unique effects of DA on pericyte biology and vascular development. Alternatively, the rapid cAMP flux associated with NE (but not with DA or NE plus DA treatment; Figure 4B, 10 minutes) may contribute to differential effects.

The use of two PKA inhibitors and a PKA activator confirmed the involvement of PKA in the DA-mediated effect on pericytes. Focal adhesion kinase (FAK) is an important regulator of signaling processes between the extracellular matrix and tumor cells [33,34]. PKA-mediated FAK phosphorylation can stimulate the binding of FAK to Src kinase and the formation of the FAK-Src complex. At focal adhesion sites, FAK activation enhances cytoskeletal reorganization, cellular adhesion, and cell survival [35,36]. In addition, FAK also promotes tumor cell migration and invasion [37]. These findings suggest that FAK activation promotes pericyte recruitment and might be involved in the DA stimulatory effect on pericytes. During

DA treatment, FAK activation could occur through either increased cAMP levels or activated PKA, leading to increased pericyte coverage of tumor vessels. In summary, we have shown that DA effectively blocks the deleterious effects of chronic stress on tumor vasculature. The antiangiogenic and pro-vessel maturation effects of DA make this catecholamine an attractive choice to improve the efficacy of therapies for cancer and other diseases with abnormal vasculature.

Acknowledgments

References
[1] Schmidt C and Kraft K (1996). Beta-endorphin and catecholamine concentrations during chronic and acute stress in intensive care patients. *Eur J Med Res* **1**, 528–532.

[2] Lutgendorf SK (2009). Depression, social support, and beta-adrenergic transcription control in human ovarian cancer. *Brain Behav Immun* **23**, 176–183.

[3] Thaker PH, Han LY, Kamat AA, Arevalo JM, Takahashi R, Lu C, Jennings NB, Armaiz-Pena G, Bankson JA, Ravoori M, et al. (2006). Chronic stress promotes tumor growth and angiogenesis in a mouse model of ovarian carcinoma. *Nat Med* **12**, 939–944.

[4] Basu S, Nagy JA, Pal S, Vasile E, Eckelhoefer IA, Bliss VS, Manseau EJ, Dasgupta PS, Dvorak HF, and Mukhopadhyay D (2001). The neurotransmitter dopamine inhibits angiogenesis induced by vascular permeability factor/vascular endothelial growth factor. *Nat Med* **7**, 569–574.

[5] Teunis MA, Kavelaars A, Voest E, Bakker JM, Ellenbroek BA, Cools AR, and Heijnen CJ (2002). Reduced tumor growth, experimental metastasis formation, and angiogenesis in rats with a hyperreactive dopaminergic system. *FASEB J* **16**, 1465–1467.

[6] Chakroborty D, Sarkar C, Basu B, Dasgupta PS, and Basu S (2009). Catecholamines regulate tumor angiogenesis. *Cancer Res* **69**, 3727–3730.

[7] Chakroborty D, Chowdhury UR, Sarkar C, Baral R, Dasgupta PS, and Basu S (2008). Dopamine regulates endothelial progenitor cell mobilization from mouse bone marrow in tumor vascularization. *J Clin Invest* **118**, 1380–1389.

[8] Moreno-Smith M, Lu C, Shahzad MM, Pena GN, Allen JK, Stone RL, Mangala LS, Han HD, Kim HS, Farley D, et al. (2011). Dopamine blocks stress-mediated ovarian carcinoma growth. *Clin Cancer Res* **17**, 3649–3659.

[9] Chantrain CF, Henriet P, Jodele S, Emonard H, Feron O, Courtoy PJ, DeClerck YA, and Marbaix E (2006). Mechanisms of pericyte recruitment in tumour angiogenesis: a new role for metalloproteinases. *Eur J Cancer* **42**, 310–318.

[10] Buick RN, Pullano R, and Trent JM (1985). Comparative properties of five human ovarian adenocarcinoma cell lines. *Cancer Res* **45**, 3668–3676.

[11] Yoneda J, Kuniyasu H, Crispens MA, Price JE, Bucana CD, and Fidler IJ (1998). Expression of angiogenesis-related genes and progression of human ovarian carcinomas in nude mice. *J Natl Cancer Inst* **90**, 447–454.

[12] Langley RR, Ramirez KM, Tsan RZ, Van Arsdall M, Nilsson MB, and Fidler IJ (2003). Tissue-specific microvascular endothelial cell lines from *H-2K^b-tsA58* mice for studies of angiogenesis and metastasis. *Cancer Res* **63**, 2971–2976.

[13] Verschraegen CF, Kumagai S, Davidson R, Feig B, Mansfield P, Lee SJ, Maclean DS, Hu W, Khokhar AR, and Siddik ZH (2003). Phase I clinical and pharmacological study of intraperitoneal *cis*-bis-neodecanoato(*trans-R, R*-1, 2-diaminocyclohexane)-platinum II entrapped in multilamellar liposome vesicles. *J Cancer Res Clin Oncol* **129**, 549–555.

[14] Siddik ZH, Boxall FE, and Harrap KR (1987). Flameless atomic absorption spectrophotometric determination of platinum in tissues solubilized in hyamine hydroxide. *Anal Biochem* **163**, 21–26.

[15] Livak KJ and Schmittgen TD (2001). Analysis of relative gene expression data using real-time quantitative PCR and the $2^{-\Delta\Delta CT}$ method. *Methods* **25**, 402–408.

[16] Sood AK, Bhatty R, Kamat AA, Landen CN, Han L, Thaker PH, Li Y, Gershenson DM, Lutgendorf S, and Cole SW (2006). Stress hormone–mediated invasion of ovarian cancer cells. *Clin Cancer Res* **12**, 369–375.

[17] Landen CN, Merritt WM, Mangala LS, Sanguino AM, Bucana C, Lu C, Lin YG, Han LY, Kamat AA, Schmandt R, et al. (2006). Intraperitoneal delivery of liposomal siRNA for therapy of advanced ovarian cancer. *Cancer Biol Ther* **5**, 1708–1713.

[18] Landen CN Jr, Lu C, Han LY, Coffman KT, Bruckheimer E, Halder J, Mangala LS, Merritt WM, Lin YG, Gao C, et al. (2006). Efficacy and antivascular effects of EphA2 reduction with an agonistic antibody in ovarian cancer. *J Natl Cancer Inst* **98**, 1558–1570.

[19] Armaiz-Pena GN, Allen JK, Cruz A, Stone RL, Nick AM, Lin YG, Han LY, Mangala LS, Villares GJ, Vivas-Mejia P, et al. (2013). Src activation by β-adrenoreceptors is a key switch for tumour metastasis. *Nat Commun* **4**, 1403–1413.

[20] Lu C and Sood AK (2008). Role of pericytes in angiogenesis. In *Angiogenesis Agents in Cancer Therapy* (2nd ed), BA Teicher and LM Ellis (Eds). Totowa, NJ, Humana Press, Inc. pp. 117–132.

[21] Siddik ZH, Jones M, Boxall FE, and Harrap KR (1988). Comparative distribution and excretion of carboplatin and cisplatin in mice. *Cancer Chemother Pharmacol* **21**, 19–24.

[22] Jain RK (2003). Molecular regulation of vessel maturation. *Nat Med* **9**, 685–693.

[23] Fiedler U and Augustin HG (2006). Angiopoietins: a link between angiogenesis and inflammation. *Trends Immunol* **27**, 552–558.

[24] Chakroborty D, Sarkar C, Yu H, Wang J, Liu Z, Dasgupta PS, and Basu S (2011). Dopamine stabilizes tumor blood vessels by up-regulating angiopoietin 1 expression in pericytes and Kruppel-like factor-2 expression in tumor endothelial cells. *Proc Natl Acad Sci USA* **108**, 20730–20735.

[25] Jain RK (2005). Normalization of tumor vasculature: an emerging concept in antiangiogenic therapy. *Science* **307**, 58–62.

[26] Winkler F, Kozin SV, Tong RT, Chae SS, Booth MF, Garkavtsev I, Xu L, Hicklin DJ, Fukumura D, di Tomaso E, et al. (2004). Kinetics of vascular normalization by VEGFR2 blockade governs brain tumor response to radiation: role of oxygenation, angiopoietin-1, and matrix metalloproteinases. *Cancer Cell* **6**, 553–563.

[27] Xian X, Hakansson J, Stahlberg A, Lindblom P, Betsholtz C, Gerhardt H, and Semb H (2006). Pericytes limit tumor cell metastasis. *J Clin Invest* **116**, 642–651.

[28] Edelman AM, Blumenthal DK, and Krebs EG (1987). Protein serine/threonine kinases. *Annu Rev Biochem* **56**, 567–613.

[29] Gonzalez GA and Montminy MR (1989). Cyclic AMP stimulates somatostatin gene transcription by phosphorylation of CREB at serine 133. *Cell* **59**, 675–680.

[30] Iyengar R (1996). Gating by cyclic AMP: expanded role for an old signaling pathway. *Science* **271**, 461–463.

[31] Lamb NJ, Fernandez A, Conti MA, Adelstein R, Glass DB, Welch WJ, and Feramisco JR (1988). Regulation of actin microfilament integrity in living nonmuscle cells by the cAMP-dependent protein kinase and the myosin light chain kinase. *J Cell Biol* **106**, 1955–1971.

[32] Yasumura Y, Buonassisi V, and Sato G (1966). Clonal analysis of differentiated function in animal cell cultures. I. Possible correlated maintenance of differentiated function and the diploid karyotype. *Cancer Res* **26**, 529–535.

[33] Schlaepfer DD, Hauck CR, and Sieg DJ (1999). Signaling through focal adhesion kinase. *Prog Biophys Mol Biol* **71**, 435–478.

[34] Schaller MD (2001). Biochemical signals and biological responses elicited by the focal adhesion kinase. *Biochim Biophys Acta* **1540**, 1–21.

[35] Sieg DJ, Hauck CR, Ilic D, Klingbeil CK, Schaefer E, Damsky CH, and Schlaepfer DD (2000). FAK integrates growth-factor and integrin signals to promote cell migration. *Nat Cell Biol* **2**, 249–256.

[36] Frisch SM, Vuori K, Ruoslahti E, and Chan-Hui PY (1996). Control of adhesion-dependent cell survival by focal adhesion kinase. *J Cell Biol* **134**, 793–799.

[37] Sood AK, Coffin JE, Schneider GB, Fletcher MS, DeYoung BR, Gruman LM, Gershenson DM, Schaller MD, and Hendrix MJ (2004). Biological significance of focal adhesion kinase in ovarian cancer: role in migration and invasion. *Am J Pathol* **165**, 1087–1095.
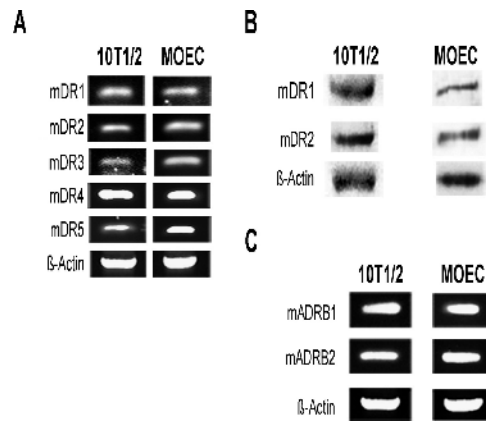
Figure W1. Expression of DA and β-adrenergic receptors in murine pericyte 10T1/2 cells and MOEC. (A) RT-PCR analysis of mDR1 to mDR5. (B) Protein expression of DR1, DR2 in pericytes, and MOEC. (C) RNA expression of β-adrenergic receptors in pericytes and MOEC.
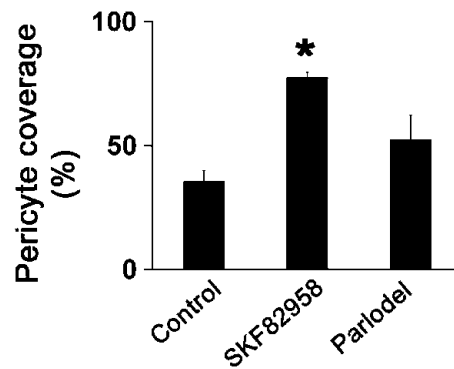

Figure W2. Pericyte coverage of SKOV3ip1 tumor endothelial cells. Tumor tissues from mice treated with DA and SKF 82958 showed significantly higher percentage of pericyte coverage compared to the control group (*$P < .0001$). Tumor tissues from mice treated with parlodel showed an increase in pericyte coverage; however, this increase was not statistical significant compared to controls.
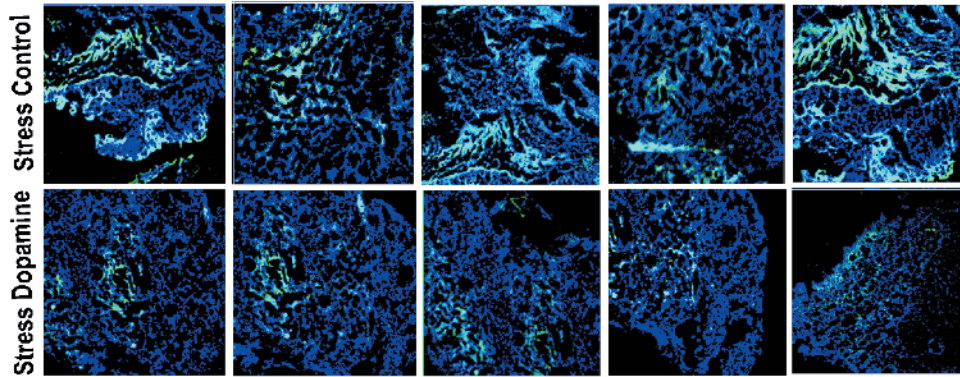
Figure W3. Hypoxic areas in ovarian cancer tumors from stressed mice. Representative confocal images (100×) of SKOV3ip1 tumor tissues from chronically stressed mice stained for CA9 (green fluorescence). Tumors from stressed mice treated with DA (lower panel) showed decreased regions of hypoxia (green fluorescence) compared with those from control (untreated) stressed mice (upper panel).
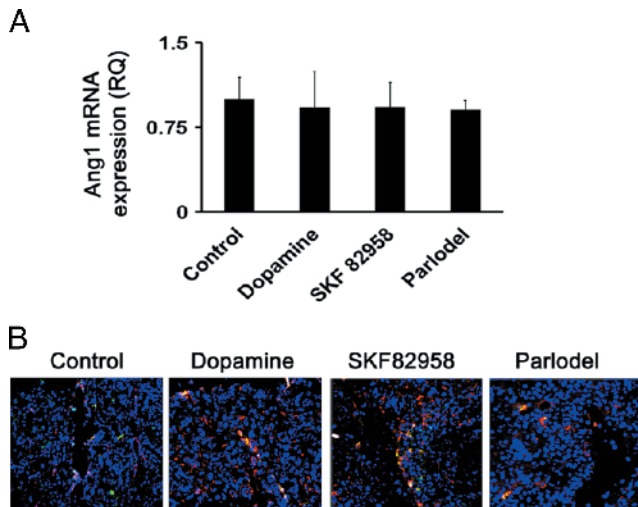

Figure W4. Ang1 expression in SKOV3ip1 tumor tissues from stressed mice. Treatments of DA, DR1 agonist SKF 82958, and DR2 agonist parlodel did not affect mRNA (A) and protein (B) expression of Ang1. Ang1 mRNA was determined by quantitative RT-PCR. Ang1 protein was detected in tumor pericytes by a double immunofluorescence staining for Ang1 (green fluorescence) and RGS5 (as pericyte marker; red fluorescence).
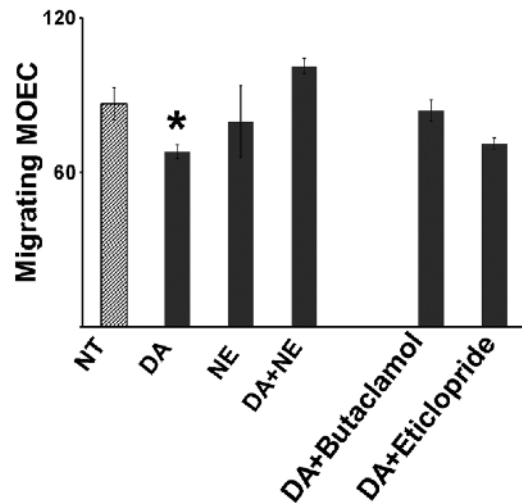
Figure W5. Migration of MOECs in the presence of DA, NE, and DA antagonist. DA exposure resulted in a 22% ($P < .05$) decrease in MOEC migration. This effect, however, was not significantly abolished with either combined treatment of DA and DR1 antagonist butaclamol (DA/butaclamol) or combined treatment of DA and DR2 antagonist eticlopride (DA/eticlopride). MOEC migration was not significantly affected by treatment with NE or DA + NE.